AIP Journal of Applied Physics

# Growth behavior of nanocrystalline diamond films on ultrananocrystalline diamond nuclei: The transmission electron microscopy studies

Chuan-Sheng Wang, Huang-Chin Chen, Hsiu-Fung Cheng, and I-Nan Lin

Citation: Journal of Applied Physics **105**, 124311 (2009); doi: 10.1063/1.3153957

View online: http://dx.doi.org/10.1063/1.3153957

View Table of Contents: http://scitation.aip.org/content/aip/journal/jap/105/12?ver=pdfcov

Published by the AIP Publishing



# Growth behavior of nanocrystalline diamond films on ultrananocrystalline diamond nuclei: The transmission electron microscopy studies

Chuan-Sheng Wang,[1,2] Huang-Chin Chen,[1] Hsiu-Fung Cheng,[3,a)] and I-Nan Lin[1]
[1]*Department of Physics, Tamkang University, Tamsui 251, Taiwan, Republic of China*
[2]*Technology and Science Institute of Northern Taiwan, Peitou, 112 Taipei, Taiwan, Republic of China*
[3]*Department of Physics, National Taiwan Normal University, Taipei 116, Taiwan, Republic of China*

(Received 4 April 2009; accepted 16 May 2009; published online 26 June 2009)

Micron-crystalline diamond (MCD) films with a unique microstructure were synthesized using a modified nucleation and growth process, in which a thin layer of ultrananocrystalline diamond (UNCD) was used as nucleation layer for growing diamond films in $H_2$-plasma. Thus obtained $(MCD)_{UNCD}$ diamond films consist of nanosized diamond clusters (~10 nm in size) surrounding the large diamond grains (~300 nm in size), exhibiting better electron field emission (EFE) properties than the conventional diamond materials with faceted grains. The EFE of these $(MCD)_{UNCD}$ films can be turned on at $E_0=11.1$ V/$\mu$m, achieving EFE current density as large as $(J_e)=0.7$ mA/cm$^2$ at 25 V/$\mu$m applied field, which can be attributed to the presence of large proportion of UNCD grains lying in between the MCD grains, forming an electron conduction path and thus facilitating the EFE process. Transmission electron microscopy examinations reveal that such a unique microstructure was formed by agglomeration and coalescence of the nanosized UNCD grains. © *2009 American Institute of Physics*. [DOI: 10.1063/1.3153957]

## I. INTRODUCTION

Diamond and related materials have enormous potential applications due to their marvelous physical and chemical properties.[1–3] Diamond films which possess good electron field emission (EFE) properties can potentially be applied as materials for fabricating electron field emitters. There are substantial researches carried out on the growth, properties, and applications of single-crystalline and microcrystalline diamond (MCD) in the past few decades. Recently, main focus has been directed toward the synthesis and properties of nanocrystalline diamond (NCD) and ultrananocrystalline diamond (UNCD) films.[4] The UNCD film possesses many excellent properties and several of them actually exceed those of diamond.[5,6] As the grain size in UNCD film is less than 10 nm, surface smoothness increases markedly making it a promising material for device applications. Additionally, the decrease in diamond grain size increases the grain boundaries containing nondiamond carbon in the film, resulting in significant improvement in electrical properties. A very high EFE characteristic has been reported from UNCD films.[7–10] In previous paper,[11] we used a modified nucleation and growth process, which utilized a layer of UNCD as nuclei, successfully synthesized a diamond film with very unique granular structure in $H_2/CH_4$ (1%) plasma, viz., the large-grain diamond contain abundant nanosized clusters on top surface. Such a unique diamond materials exhibit markedly better EFE properties than the conventional diamond films with faceted grains grown on bias enhanced nuclei. However, the control of the processing parameters for obtaining such a unique microstructure is very stringent and how such a granular structure was formed is not clear.

In this paper, the detailed microstructure of these MCD materials grown on UNCD nuclei was examined by using transmission electron microscopy (TEM) and the microstructure development model was proposed based on the observations.

## II. EXPERIMENTAL

The UNCD, instead of bias-enhanced-nucleated seeds, was used as nucleation layer to promote the growth of diamonds on *n*-type mirror polished Si (100) substrates. To form UNCD nucleation layer on Si substrates, the substrates were first treated by ultrasonication in a solution containing diamond powders (~1 nm) for 30 min and were ultrasonically cleaned by acetone to remove any adhered particles. The diamond nuclei were then formed by the microwave plasma enhanced chemical vapor deposition (CVD) process in $Ar/CH_4$ (1%) plasma for 20 min, using an IPLAS CYRANNUS-I system. Figure 1(a) shows the SEM micrograph of the UNCD seeding layer, which consists of ultrasmall clusters. The TEM micrograph of these UNCD seeding layer [Fig. 1(b)], along with the selected area electron diffraction (SAED) pattern and the structure image [insets, Fig. 1(b)], reveals that the clusters contained in the seeding layer are ultrasmall diamond grains (~5 nm) with very uniform size distribution. Growths of diamonds were carried out in a microwave plasma enhanced CVD processor (2.45 GHz, ASTeX 5400) with 1%$CH_4/H_2$, 73 mbars for 60 min. Thus obtained diamond films were designated as $MCD_{UNCD/Si}$ films and those grown directly on biased-enhanced-nucleation (BEN)-treated Si substrates were designated as UNCD/Si films.

Surface morphology of nanodiamond films was examined using a field emission scanning electron microscope (SEM) (VEGA-TESCAN). Microstructure of the films was

a)Author to whom correspondence should be addressed. Electronic mail: hfcheng@phy03.phy.ntnu.edu.tw.

 

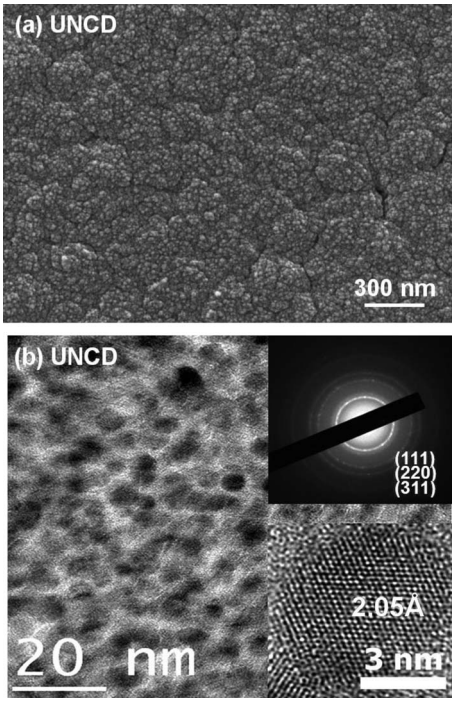


FIG. 1. The (a) SEM micrographs and (b) TEM micrographs of UNCD layer grown Si substrates using $CH_4(1\%)/Ar$-plasma. The UNCD layer was used as the seeding for growing the MCD diamond films in $CH_4(1\%)/H_2$-plasma.

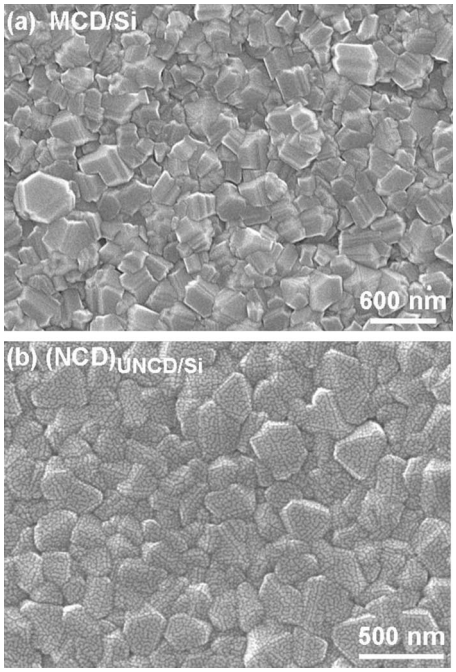


FIG. 2. The SEM micrographs of (a) MCD diamond films prepared by conventional CVD process on ultrasonicated Si substrates and (b) $(MCD)_{UNCD/Si}$ diamond films prepared by modified CVD process on UNCD seeding layer.

examined using TEM (JEOL, JEM2100F). Crystal quality of nanodiamond films was investigated by Raman spectroscopy using 514.5 nm argon laser beam (Renishaw). EFE properties of the diamond films were measured with a tunable parallel plate setup, in which the sample-to-anode distance was controlled using a micrometer. The current-voltage (*I-V*) characteristics were measured using an electrometer (Keithley 237) under pressures below $10^{-6}$ mbar. The EFE parameters were extracted from the obtained *I-V* curves by using the Fowler–Nordheim (FN) model.[12] The maximum available voltage of the setup is 1100 V, and the current was restricted to 10 mA. The turn-on field ($E_0$) was designated as the intersection of the lines extrapolated from the low field and high field segments of the FN plot.

## III. RESULTS AND DISCUSSION

Figure 2(a) shows the SEM micrograph of the diamond films grown directly on the Si substrates (MCD/Si), which were seeded by BEN process,[13] indicating that the MCD/Si films contain large faceted grains, about 0.4 $\mu$m. The MCD/Si films usually require high field to turn on the EFE properties, i.e., with $(E_0)_{MCD}=40.1$ V/$\mu$m, achieving EFE current density about $(J_e)_{MCD}=2.75$ mA/cm$^2$ at 88.0 V/$\mu$m applied field.[13] In contrast, Fig. 2(b) illustrates that the diamond films grown by the modified CVD process posses a tremendously different microstructure. The $(MCD)_{UNCD/Si}$ films contain grains about 0.3 $\mu$m in size, which is of similar size with the grains in conventional MCD/Si diamond films. The SEM micrographs reveal that the large grains actually consist of ultrasmall clusters, which is about one-fifth in size.

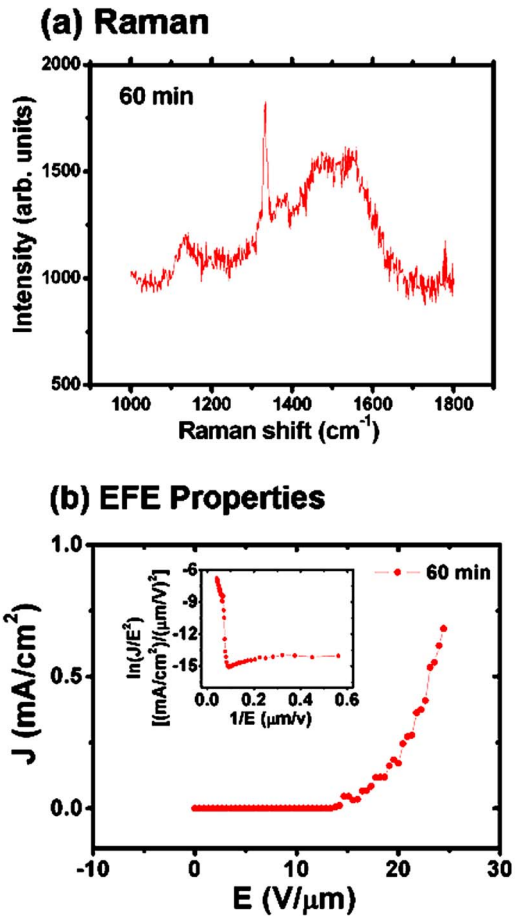


FIG. 3. (Color online) (a) Raman spectroscopy and (b) EFE properties of the $(MCD)_{UNCD/Si}$ diamond films.

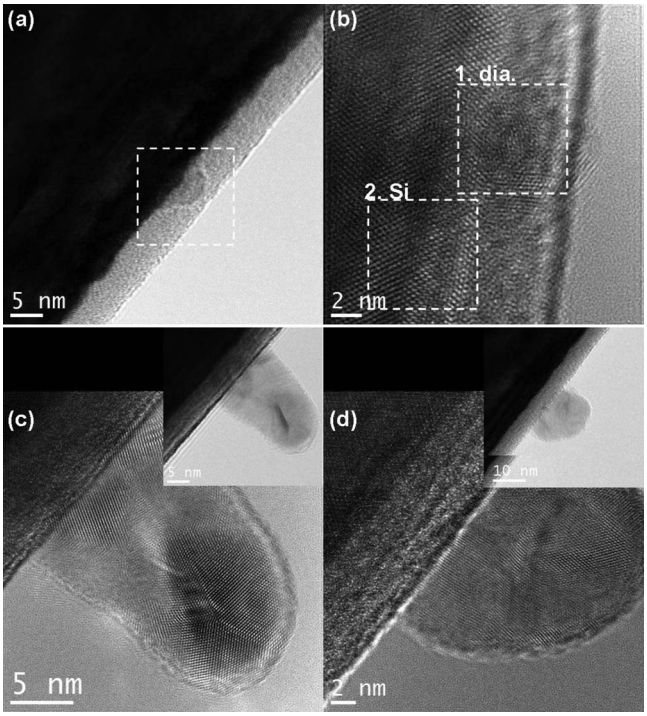


FIG. 4. (a) Typical cross-sectional TEM micrographs and (b) the structural image of the designated area in "a" of the $(NCD)_{UNCD/Si}$ diamond films, showing that the nuclei formed heterogeneously from the amorphous carbon-to-Si interface; [(c) and (d)] some typical structure images of the UNCD grains grown from the amorphous carbon-to-Si interface.

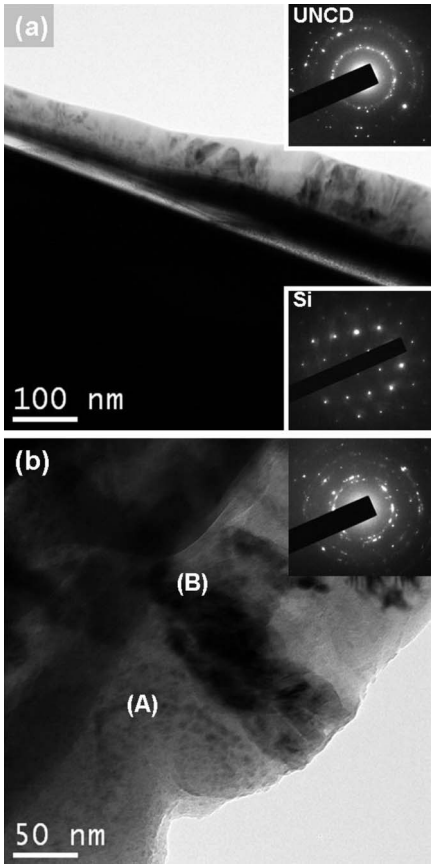


FIG. 5. Typical (a) cross-sectional TEM micrographs and (b) the enlarged TEM micrographs of some region of the $(MCD)_{UNCD/Si}$ diamond films.

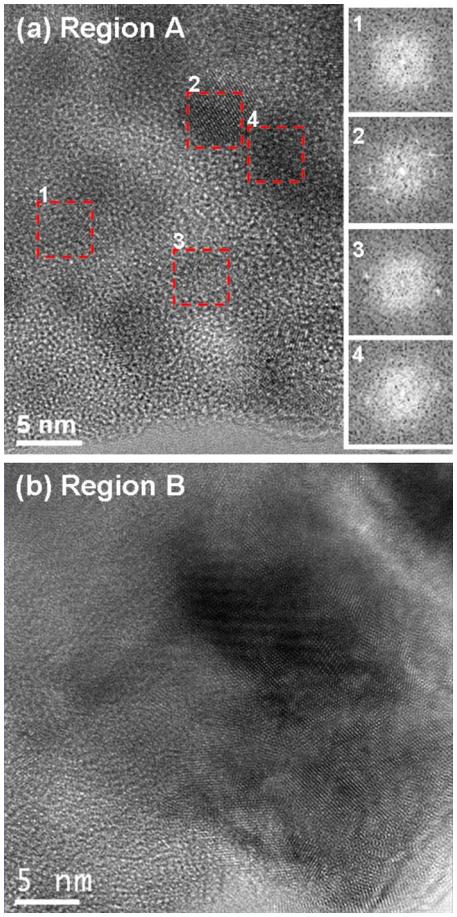


FIG. 6. (Color online) Structure images of (a) region A and (b) region B of the cross-sectional TEM micrographs of the $(MCD)_{UNCD/Si}$ diamond films shown in "Fig. 5(b)."

Raman spectra in Fig. 3(a) indicate that the $(MCD)_{UNCD/Si}$ films possess similar Raman structure with those of MCD/Si films, that is, there appears a sharp Raman peak at 1332 $cm^{-1}$, the signature of the large-grain diamond materials. In addition, there also exist broaden Raman resonance peaks, the signature of UNCD films.[14] The $\upsilon_1$-band in the vicinity of 1140 $cm^{-1}$ and $\upsilon_2$-bands in the vicinity of 1480 $cm^{-1}$ indicate the presence of ultrasmall $sp^3$-bonded

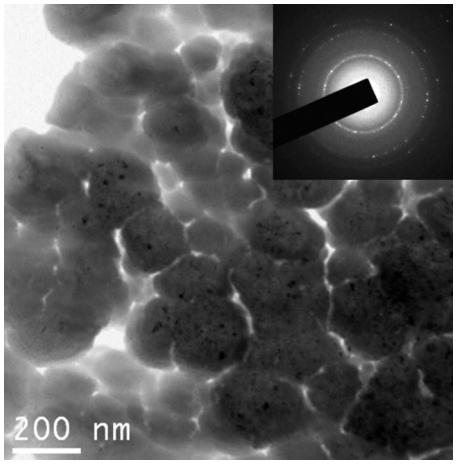


FIG. 7. The TEM micrographs of NCD (MCD) grown on UNCD nuclei, using $CH_4(1\%)/H_2$-plasma, where the UNCD nuclei were grown on Si using $CH_4(1\%)/Ar$-plasma.

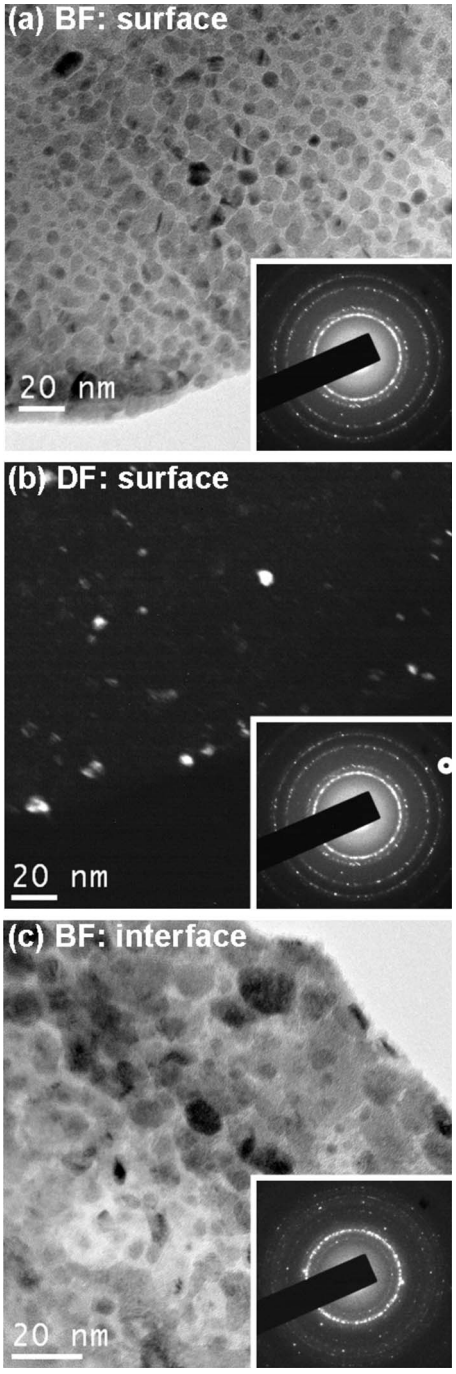


FIG. 8. (a) Bright field (BF) and (b) DF TEM micrographs of the surface region, and (c) the BF of the interface region of the $(MCD)_{UNCD/Si}$ diamond films with the insets showing the SAED patterns of the corresponding micrographs.

diamond grains and *trans*-polyacetelyne phase.[14] There also appears $D^*$-band near 1350 $cm^{-1}$ and $G$-band near 1580 $cm^{-1}$,[15] indicating the presence of disordered carbons and graphitic phases, respectively. These Raman spectrum implies that the $(MCD)_{UNCD/Si}$ films posses both the characteristics of MCD and UNCD films. Figure 3(b) illustrates that these $(MCD)_{UNCD/Si}$ films possess markedly better EFE behavior than the MCD/Si films. The EFE process of $(MCD)_{UNCD/Si}$ films can be turned on at $(E_0)_{NCD/UNCD/Si}$ $=11.1$ $V/\mu m$ and achieve a large EFE current density of $(J_e)_{MCD/UNCD/Si}=0.7$ $mA/cm^2$ at 25.0 $V/\mu m$ applied field.

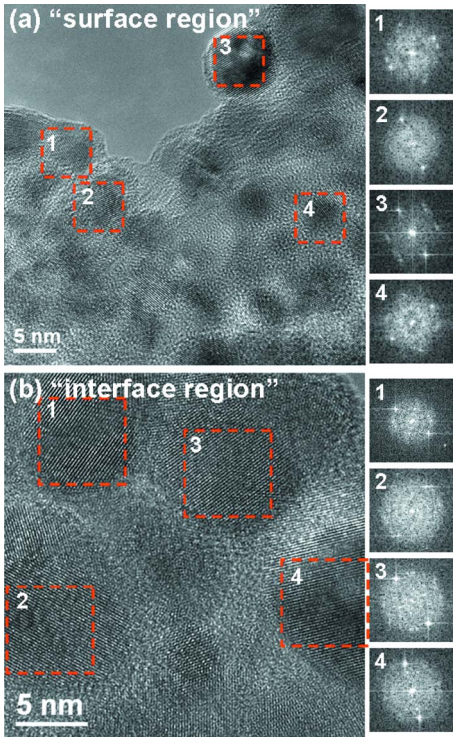


FIG. 9. (Color online) The structure image of (a) the surface region and (b) the interface region of the $(MCD)_{UNCD/Si}$ diamond films, where the Fourier transformed images show that the grains are diamonds.

It should be noted that conventional MCD/Si films are essentially nonemitting at such an applied field.

To understand how the unique granular structure of $(MCD)_{UNCD/Si}$ films was formed, the detailed microstructure of these samples was examined using TEM. For the first, the characteristics of UNCD seeding layer were investigated. Typical cross-sectional microstructure of an UNCD seeding layer shown in Fig. 4 reveals the onset of the nucleation process. Figure 4(a) shows that a thin layer of amorphous carbons was formed first and the UNCD grains nucleated heterogeneously at the amorphous-to-Si interface rather than homogeneously inside the amorphous layer. Such a phenomenon is understandable, as the heterogeneous nucleation process is always energetically favorable, as compared to the homogeneous nucleation one. The structure image shown in Fig. 4(b) implies that the orientation of UNCD nuclei is not correlated with that of the Si material. Figures 4(c) and 4(d) illustrate two examples of the UNCD particles grown from the nuclei, revealing that the UNCD particles contain multiple grains. These observations confirm that the diamonds renucleate easily on the existing grains, resulting in polycrystalline UNCDs, at the presence of $C_2$ dimers. On contrary, for the growth of diamonds in $CH_4/H_2$ plasma, the $CH_3^+$ methyl radicals can only form $sp^3$-bonds on the existing diamond surface, enlarging the size of the grains and leading to large grain diamond films.

Figure 5(a) shows the typical cross-sectional micrograph of $(MCD)_{UNCD/Si}$ films, revealing the existence of a very thin interface between the diamond films and the Si substrate. Figure 5(b) shows the enlarged microstructure of the region near the MCD-to-Si substrate. The SAED (inset) reveal that

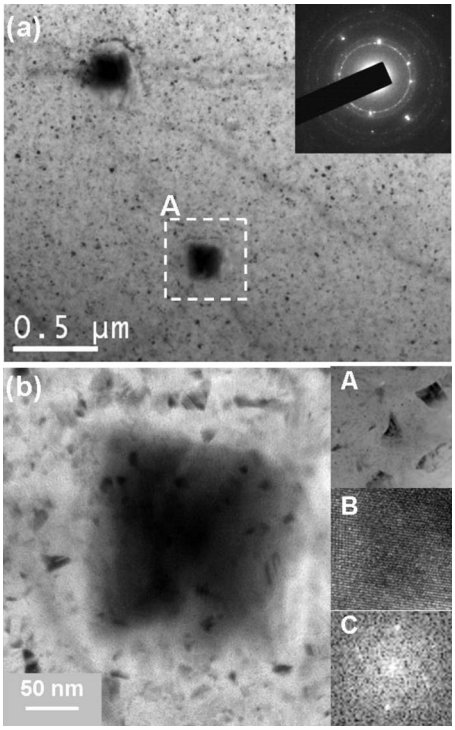


FIG. 10. (a) The plan-view TEM micrographs of a typical area of the interface region of the $(MCD)_{UNCD/Si}$ diamond films and (b) the enlarged micrograph of region A in a, where inset A shows the enlarged micrographs and inset B shows the structure image of some area near the large grains; inset C shows the Fourier transformed image of inset B.

all the materials are diamonds. In some regions (e.g., area A), there exist abundant nanosized clusters. Structure image shown in Fig. 6(a) and the associated Fourier transformed images confirm that the small clusters contained in area A are UNCD grains. In other regions (e.g., area B), there appear large clusters. The structure image shown in Fig. 6(b) reveals that the large clusters in area B are polycrystalline diamonds, which contain randomly oriented diamond grains. The large diamond cluster grew directly from the interface, coexisting with the region containing small clusters, rather then grew on top of the UNCD seedings.

It should be reminded that the MCD films were grown using $CH_4/H_2$ plasma, instead of $CH_4/Ar$ plasma. It is believed that the abundant atomic hydrogen produced in $CH_4/H_2$ plasma can efficiently etch the *trans*-polyacetylene layer surrounding the UNCD grains in seeding layer. Without the passivation of the *trans*-polyacetylene layer, the nanosized diamond grains agglomerate easily, which coalescence later on to form large single-crystalline diamond grain. Probably, the coalescence started at the center of agglomerates, resulting in a microstructure that the center is a large single-crystalline grain and the surrounding are uncoalesced UNCD grains. Moreover, there are abundant nanosized grains existing in between the coalesced large grains. The above-described observations infer that the large diamond grains were formed first by agglomeration of the small diamonds grains, followed by the coalescence of small diamond grains.

To investigate the formation mechanism of the unique microstructure of the $(MCD)_{UNCD/Si}$ diamond films, a thin foil representing the microstructure of the surface region of the $(MCD)_{UNCD/Si}$ samples was prepared by ion milling from the Si substrates. Figure 7 shows the typical plan-view TEM micrograph of the $(MCD)_{UNCD/Si}$ thin films of the surface region revealing that the samples contain the agglomerates around 200–400 nm in size and uniform in size distribution. Figure 8(a) shows the detail microstructure of the agglomerates in the surface region, indicating that each agglomerate contains many ultrasmall clusters about 5–10 nm in size. The SAED shown as inset in this figure indicates that these small clusters are of diamond structure, i.e., they are UNCD grains.

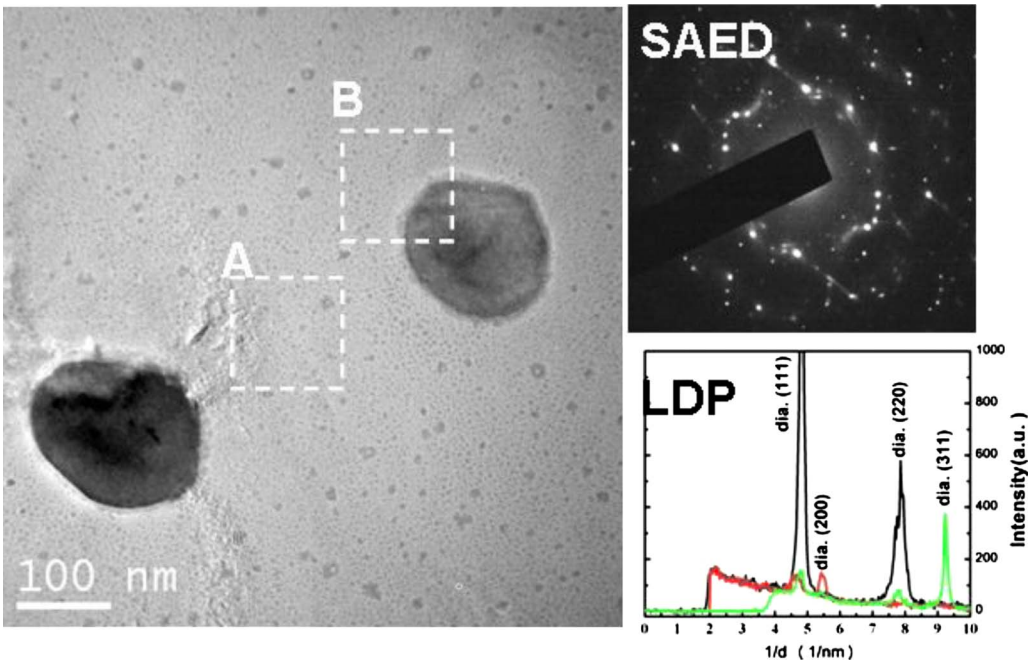


FIG. 11. (Color online) The plan-view TEM micrographs of another area of the interface region of the $(MCD)_{UNCD/Si}$ diamond films, where the insets are the SAED patterns and the LDP extracted from the SAED.

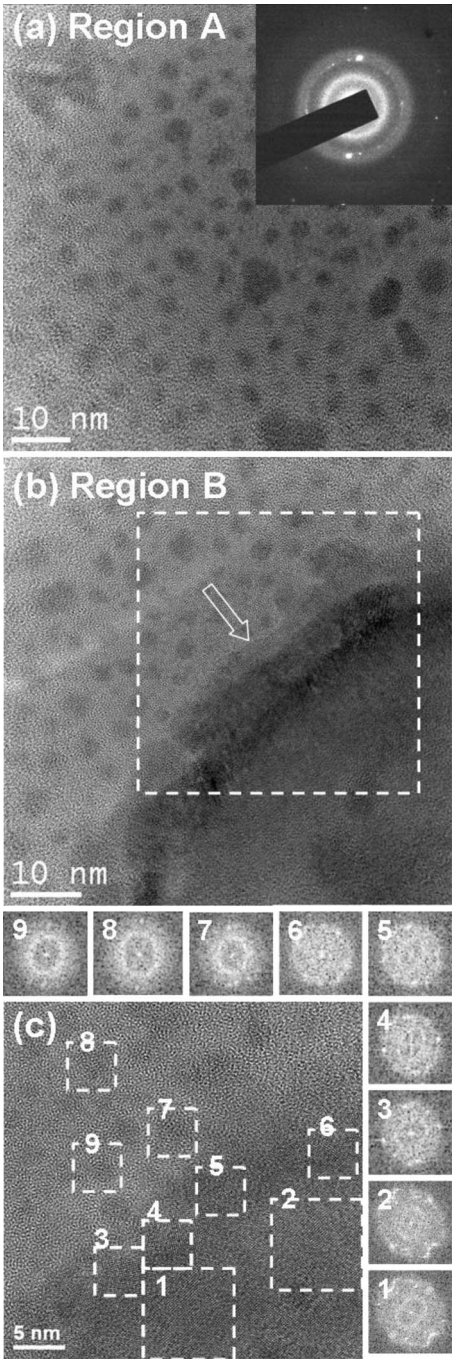


FIG. 12. (a) The enlarged micrograph and the SAED (inset) of region A of the $(MCD)_{UNCD/Si}$ diamond films in "Fig. 11," (b) the structure image of region B of the $(MCD)_{UNCD/Si}$ diamond films in Fig. 11 showing the presence of an interface surrounding the large diamond grains; and (c) the structure image of designated region in "b," where the Fourier transformed images 1 and 2 show that they are diamonds of the same grains, Fourier transformed images 3–6 show that they are different diamond grains surrounding the interface and the those of 7–9 are diamonds embedded in amorphous carbons.

Typical dark field (DF) image of this area [Fig. 8(b)] further confirms that the SAED rings are contributed from the equiaxed UNCD grains in these large agglomerates. Figure 9(a) reveals the structure image of the typical region in Fig. 8(a), which, in conjunction with the Fourier transformed images for the designated areas, further illustrate that the grains are of diamond structure. It should be mentioned that the thin foil actually represents the top most layer of the $(MCD)_{UNCD/Si}$ thin films. No structural image of the underlying MCD grains was observable in these micrographs.

Secondarily, thin foils representing the region in the vicinity of the MCD-to-UNCD/Si interface were prepared, that is, the Si substrate materials were etched away chemically and the TEM samples were prepared by ion milling the diamond films from the diamond surface. Thus obtained samples are designated as "interface region." Figure 8(c) shows the typical plan-view microstructure of the interface region, which, in conjunction with the SAED of this region (inset), illustrates that the microstructure of this interface region is similar with those of the surface region of the $(MCD)_{UNCD/Si}$ samples, viz., it contains diamonds structure with grains size around 5–10 nm. However, detailed investigation on the SAED reveals that the diamonds are *n*-diamond[16] with fcc structure, instead of *c*-diamond with diamond structure. The structural image (and the associated Fourier transformed images) shown in Fig. 9(b) further confirms that the small clusters are *n*-diamonds, rather than the *c*-diamonds. Moreover, in the interface region, it is frequently observed that, in addition to the ultrasmall equiaxes grains, there also exist large clusters that are scarcely distributed among the ultrasmall clusters in the films [Fig. 10(a)]. The SAED pattern [inset, Fig. 10(a)] contains spotty patterns contributed from large diamond crystals and ring patterns contributed from randomly oriented ultrasmall diamond grains. Figure 10(b) shows the TEM micrograph in higher magnification for region A in Fig. 10(a). Typical enlarged micrograph of the region adjacent the large diamond grains, shown as inset A in Fig. 10(b), in conjunction with the structure image [inset B, Fig. 10(b)] and Fourier transformed image [inset C, Fig. 10(b)], indicates that this region contains nanosized diamonds coexisting with large grains.

Figure 11(a) illustrates another example of the similar microstructure, that is, the samples contain large clusters distributed among the ultrasmall clusters. The SAED patterns (inset, Fig. 11) and the associated linear diffraction pattern (LDP) (inset in Fig. 11) reveal again that the materials in this area are also *n*-diamond. Figure 12(a) shows the enlarged TEM micrograph of region A in Fig. 11. The SAED shown as inset in this figure indicates that in addition to the sharp rings corresponding to nanosized diamond clusters, there also appear diffuse rings, corresponding to amorphous phase. That is, this area mainly contains nanosized diamond particles embedded in amorphous carbons matrix.

Figure 12(b) illustrates the enlarged micrograph of the region in the vicinity of large clusters (region B, Fig. 11), revealing that there exists an intermediate layer about 5–10 nm in thickness lying in between the large clusters and the adjacent region [arrow, Fig. 12(b)]. Figure 12(c) shows the structural micrograph of the designated area in Fig. 12(b). The lattice image in areas "1" and "2" and the corresponding Fourier transformed images reveal that they are diamonds of the same orientation, implying that they are of the same grains, viz., the large cluster is a single diamond grain. In contrast, the lattice image and the corresponding Fourier transformed images for areas "3–6," lying in the intermediated layer, indicate that they are randomly oriented dia-

monds, viz., the intermediated layer contains nanosized diamond grains with random orientation. The lattice image and the corresponding Fourier transformed images for areas "7–9" infer that they are nanosized diamond embedded in amorphous carbons. These micrographs strongly infer that the large diamond grains were formed by the Ostwald–Ripening process, viz., they grew with annihilation of the adjacent ultrasmall grains. Presumably, the amorphous is the carbon film formed prior to the formation of diamond nuclei in the synthesis of UNCD seeding layer (cf. Fig. 4).

It should be noted that the large grains were observable only in the interface region. No large grains were seen in the surface region. The large grains in the interface region are scarcely distributed. The micrographs observed in Figs. 10 and 11 represent the microstructures of the region very near the Si substrates. However, there are always some UNCD grains existing in between the MCD grains. Such an observation is in accord with the SEM microstructure observed in Fig. 2(b). Restated, the large MCD grains are separated by the abundant UNCD grains about a few nanometers in size. The nanosized grains existing in between the large grains form an electron conduction path and, thereafter, leads to superior EFE properties for the $(MCD)_{UNCD/Si}$, as compared to the conventional micron-sized diamond films.

## IV. CONCLUSION

TEM was utilized to investigate the formation mechanism for the unique microstructure of the MCD films grown on UNCD seeding layer. Such a $(MCD)_{UNCD/Si}$ diamond films possess a unique microstructure, in which the UNCD clusters ($\sim$10 nm in size) surround the large diamond grains ($\sim$200–300 nm in size). The $(MCD)_{UNCD/Si}$ diamond films exhibit better EFE properties than the conventional diamond materials with faceted grains. The EFE can be turned on at $E_0=11.1$ V/$\mu$m, achieving EFE current density as large as $(J_e)=0.7$ mA/cm$^2$ at 25 V/$\mu$m applied field. The superior EFE properties of the $(MCD)_{UNCD/Si}$ diamond films is attributed to the present of large proportion of UNCD grains lying in between the NCD grains that form an electron conduction path, facilitating the EFE process. TEM examinations reveal that the large diamond grains were formed by first agglomerating the UNCD grains and then followed by the coalescence process.

## ACKNOWLEDGMENTS

The authors would like to thank the National Science Council, Republic of China for the support of this research through the Project Nos. NSC 97-2112-M–003-011-MY2 and NSC 96-2112-M032-011-MY3.

[1] K. Chakrabarti, R. Chakrabarrti, K. K. Chattopadhyay, S. Chaudhrui, and A. K. Pal, Diamond Relat. Mater. **7**, 845 (1998).
[2] V. Ralchenko, A. Karabutov, I. Vlasov, V. Frolov, V. Konov, S. Gordeev, S. Zhukov, and A. Dementjev, Diamond Relat. Mater. **8**, 1496 (1999).
[3] S. G. Wang, Q. Zhan, S. F. Yoon, J. Ahn, Q. Wang, Q. Zhou, and D. J. Yang, Phys. Status Solidi A **193**, 546 (2002).
[4] D. M. Gruen, Annu. Rev. Mater. Sci. **29**, 211 (1999).
[5] J. A. Carlisle and O. Auciello, Electrochem. Soc. Interface **12**, 28 (2003).
[6] V. Mortet, O. Elmazria, M. Nesladek, M. B. Assouar, G. Vanhoyland, J. D. Haen, M. D. Olieslaeger, and P. Alnot, Appl. Phys. Lett. **81**, 1720 (2002).
[7] W. Zhu, G. P. Kochanski, and S. Jin, Science **282**, 1471 (1998).
[8] Y. C. Lee, S. J. Lin, C. T. Chia, H. F. Cheng, and I. N. Lin, Diamond Relat. Mater. **13**, 2100 (2004).
[9] D. Pradhan, Y. C. Lee, C. W. Pao, W. F. Pong, and I. N. Lin, Diamond Relat. Mater. **15**, 2001 (2006).
[10] Y. C. Lee, S. J. Lin, D. Pradhan, and I. N. Lin, Diamond Relat. Mater. **15**, 353 (2006).
[11] C. S. Wang, H. C. Chen, H. F. Cheng, and I. N. Lin, Diamond Relat. Mater. **18**, 136 (2009).
[12] R. H. Fowler and L. Nordheim, Proc. R. Soc. London, Ser. A **119**, 173 (1928).
[13] Y. C. Lee, S. J. Lin, I. N. Lin, and H. F. Cheng, J. Appl. Phys. **97**, 054310 (2005).
[14] A. C. Ferrari and J. Robertson, Phys. Rev. B **63**, 121405 (2001).
[15] R. G. Buckley, T. D. Moustakas, L. Ye, and J. Varon, J. Appl. Phys. **66**, 3595 (1989).
[16] B. G. Burkhard, K. Dan, Y. Tanabe, A. K. Sawaoka, and K. Yamada, J. Appl. Phys. **33**, 5875 (1994).